Design of an Adaptive Neuro-Fuzzy Damping Controller for Grid-Integrated Hybrid Microgrids Incorporating Wind Energy and Battery Storage Systems

kimmi kranthi kumar¹, P.Murari²

¹ PG Student, EEE & Sankethika Vidya parishad College of Engineering, Visakhapatnam
² HOD OF EEE Department, EEE & Sankethika Vidya parishad College of Engineering, Visakhapatnam

ABSTRACT

The increasing integration of renewable energy sources (RESs), such as wind turbines and photovoltaic (PV) arrays, introduces low-inertia characteristics that negatively affect the dynamic stability of modern power systems. To address this challenge, this study proposes Adaptive Neuro-Fuzzy Damping Controller (ANFDC) based on a high-voltage direct current (HVDC) link to enhance system damping and stability. The controller employs a fuzzy linguistic rule to tune its parameters, converting dynamic input signals into linguistic variables during an offline training phase. A hybrid microgrid system combining offshore and onshore wind turbines, PV units, and small-scale synchronous generators (SSSGs) is used to train and validate the controller. During real-time operation, the ANFDC adaptively adjusts control signals to mitigate oscillations without relying on an explicit system model. The proposed method effectively integrates the strengths of neural networks and fuzzy logic to achieve fast, robust, and adaptive damping control. Simulation results on a grid-connected hybrid microgrid under various short-circuit faults demonstrate that the ANFDC significantly improves damping performance and maintains high stability margins compared with conventional control approaches.

INDEX TERMS: Lowinertia resources (LIRs), high voltage direct current (HVDC), microgrid, wind turbines (WT), photovoltaic arrays (PV), small-scale synchronous generators (SSSGs), adaptive neuro-fuzzy-based damping controller (ANFDC).

I. INTRODUCTION

The increasing integration of renewable energy sources (RESs) such as wind turbines (WTs), photovoltaic (PV) systems, and small-scale synchronous generators (SSSGs) within modern power systems has led to the rapid development of microgrids. These microgrids offer environmentally friendly and sustainable alternatives to conventional fossil-fuel-based power plants. However, the

proliferation of inverter-based low inertia resources (LIRs) introduces significant challenges to the dynamic stability of power systems. The reduced system inertia due to these renewable units often results in poor damping characteristics, increased oscillations, and vulnerability to transient disturbances. Countries with access to abundant offshore and oceanic resources, including the United States, United Kingdom, Denmark, and Ireland, are increasingly utilizing offshore wind farms (OWFs) and wave energy farms (WEFs) for large-scale power generation. The integration of such variable and geographically distributed renewable sources through high-voltage direct current (HVDC) transmission systems has become an effective solution for reliable grid interconnection. Nevertheless, these HVDC-linked systems require advanced control strategies to ensure effective damping of low-frequency oscillations and to preserve system stability under varying operating conditions and fault scenarios.

To address these issues, the development of adaptive and intelligent damping controllers has gained attention. Among various intelligent control approaches, the combination of neural networks and fuzzy logic—referred to as adaptive neuro-fuzzy inference systems (ANFIS)—offers a promising solution. These systems are capable of handling nonlinearities, uncertainties, and dynamic changes in the grid, thereby improving overall damping performance and stability margins. This study focuses on the design of an adaptive neuro-fuzzy damping controller (ANFDC) integrated with an HVDC link for a grid-connected hybrid microgrid consisting of wind, solar, and synchronous resources.

II. LITERATURE REVIEW

Recent research has extensively explored various control strategies to mitigate oscillations and improve the stability of renewable-based power systems. Conventional proportional—integral—derivative (PID) controllers have been widely implemented due to their simplicity and ease of tuning. However, their performance deteriorates under nonlinear and time-varying operating conditions. Studies have shown that PID controllers are limited by high sensitivity to parameter variations, delayed responses, and the need for model-based adjustments, which make them less effective for systems with high renewable penetration. To overcome these challenges, several intelligent control methods have been proposed. Neuro-fuzzy controllers and ANFIS-based approaches have



Volume: 09 Issue: 10 | Oct - 2025 SJIF Rating: 8.586 ISSN: 2582-3930

been successfully applied in different power system applications, offering enhanced adaptability and robustness. For example, ANFIS-based controllers have been utilized to improve voltage regulation, load frequency control, and interarea oscillation damping in systems integrated with wind farms and PV units. Furthermore, the application of fuzzy logic controllers in conjunction with HVDC links has demonstrated improved damping performance uncertain dynamic conditions. Despite advancements, existing approaches often rely heavily on system models and require extensive tuning efforts. Moreover, few studies have investigated the implementation of adaptive neuro-fuzzy-based damping controllers within HVDC-linked hybrid microgrids that combine multiple renewable sources such as PV systems, OWFs, WEFs, and SSSGs. Therefore, there is a research gap in developing a non-model-based, adaptive, and real-time damping control framework capable of effectively handling the nonlinearities and uncertainties of multi-source renewable microgrids. The proposed ANFDC in this study addresses this gap by integrating fuzzy linguistic rules and neural network learning capabilities to enhance system damping through online adaptive control.

III. DETAILED STRUCTURE OF THE DEVELOPED TEST SYSTEM

The developed test system is a grid-connected microgrid that integrates multiple renewable energy resources (RESs), including offshore wind farms (OWFs), wave energy farms (WEFs), photovoltaic (PV) arrays, and small-scale synchronous generators (SSSGs). These units are interconnected through a high-voltage direct current (HVDC) link that facilitates efficient power transfer and provides controllability over dynamic behaviors within the microgrid. The overall configuration of the test system is illustrated schematically in Fig. 1 of the paper.

Each RES in the system possesses an individual dynamic model designed to represent its electromechanical and power-electronic characteristics. The following subsections describe the key components and their associated mathematical models.

A. Wind Turbine Model

The offshore wind farm consists of variable-speed wind turbines equipped with permanent magnet synchronous generators (PMSGs). The mechanical power extracted from the wind is expressed as a function of air density, rotor area, wind speed, and the turbine's power coefficient. The power coefficient $Cp(\lambda,\beta)C_p(\lambda,\beta)C_p(\lambda,\beta)$ depends on the tip speed ratio and the pitch angle of the blades. The wind turbine operates within defined speed limits—cut-in at 4 m/s, rated at 15 m/s, and cut-off at 25 m/s. The mathematical relations describe the aerodynamic conversion process and serve as the basis for analyzing turbine dynamics under different wind conditions.

B. Wave Energy Turbine Model

The WEF utilizes underwater induction generators driven by ocean wave turbines through gearboxes. The mechanical power generated is defined by the water density, turbine area, and wave velocity. Similar to wind energy conversion, the turbine's efficiency is characterized by a power coefficient dependent on the wave speed ratio and pitch angle. The model is evaluated using cut-in, rated, and cut-off speeds of 1 m/s, 2.5 m/s, and 5 m/s, respectively.

C. Permanent Magnet Synchronous Generator (PMSG) Model

The electrical characteristics of the PMSG used in the wind turbine are modeled in the d-q reference frame using Park's transformation. The stator voltage equations include both stator resistance and flux linkages in the d-q axes, while the flux components are defined in terms of the magnetizing and leakage reactances. The converter–inverter structure is controlled to regulate both reactive power and rotor speed. The HVDC voltage source converter (VSC) associated with the PMSG adjusts its output based on DC-link voltage and modulation indices to ensure smooth power injection into the grid.

D. Induction Generator Model for Wave Turbine

The induction generator dynamics for the wave energy system are formulated using d-q axis equations representing stator and rotor voltage and current relationships. The model includes stator and rotor resistances, leakage reactances, and magnetizing reactance. The electromagnetic torque is derived from the interaction of stator and rotor currents, providing a detailed representation of electromechanical energy conversion in the WEF subsystem.

E. HVDC-Link Model

The HVDC link serves as the central coupling mechanism between the various RESs and the main grid. It comprises three major components: the AC/DC converter, the DC transmission line, and the DC/AC inverter. The HVDC system is designed to maintain constant DC parameters while ensuring efficient power conversion between AC and DC domains. Control of the converter and inverter sides is achieved using either a PID or ANFIS-based damping controller, which regulates the DC current and voltage according to system dynamics. The governing equations describe converter firing angles and damping control signals that stabilize power flow during transient events.

F. Photovoltaic (PV) System Model

The PV subsystem is composed of a large array of BP272UU solar panels, each rated at 80 W with a nominal voltage of 19 V and a current of 4.4 A. To achieve higher output voltage and power, panels are connected in both series and parallel configurations, producing approximately 6.5 MW total output power. The PV array model incorporates diode characteristics, shunt resistance, and temperature-dependent current equations. A DC–AC inverter and DC-link capacitor regulate



Volume: 09 Issue: 10 | Oct - 2025 SJIF Rating: 8.586 ISSN: 2582-3930

the PV output voltage and interface it with the grid via the HVDC system. Differential equations describe current, voltage, and energy storage behavior within the PV inverter circuit.

G. Small-Scale Synchronous Generator (SSSG) Model

The microgrid also includes small synchronous generators modeled using a third-order differential representation in the d-q frame. Each generator is equipped with an IEEE Type DC1A excitation system that regulates the internal voltage and maintains steady operation under varying load and fault conditions. The model considers both transient and subtransient dynamics to capture accurate generator behavior during disturbances.

H. Summary of Test System Configuration

In the developed hybrid microgrid, the OWF, WEF, PV, and SSSG units are connected to a common AC bus, and their power is transmitted to the main grid through a coordinated HVDC link. This configuration enables high controllability, flexible operation, and enhanced dynamic performance. The comprehensive mathematical models of each subsystem are formulated primarily in per-unit (p.u.) values, while angular frequencies are represented in radians per second. These models collectively form the foundation for analyzing the system's dynamic response and for designing the proposed adaptive neuro-fuzzy damping controller in subsequent sections.

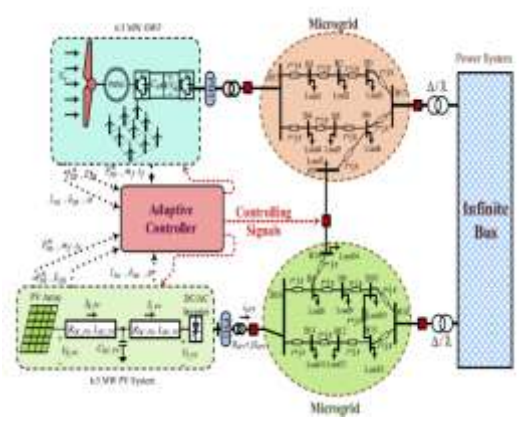


Fig 1 Single line diagram of test system consists of PV, WEF, OWF and SSSG sources connected within HVDC link.

IV. MODELING THE PROPOSED DAMPING CONTROLLER

This section presents the modeling, structure, and operating mechanism of the proposed Adaptive Neuro-Fuzzy Damping Controller (ANFDC) developed to enhance the dynamic stability of a grid-connected hybrid microgrid system. The hybrid system integrates multiple renewable energy sources (RESs) through a high-voltage direct current (HVDC) link. To verify the effectiveness of the proposed ANFDC, a conventional proportional—integral—derivative (PID) damping controller is also designed and analyzed for comparison. Both controllers are implemented within the HVDC link to generate a corrective damping signal that mitigates power oscillations and stabilizes system dynamics during disturbances and transient conditions. The overall concept of the proposed ANFIS-

based damping controller is illustrated in the system block diagram provided in the paper. The controller operates by processing dynamic input signals obtained from the microgrid, such as the speed deviation of the small-scale synchronous generators ($\Delta\omega$ SSSG) and the active power variations of the renewable sources. These input signals are analyzed to identify critical low-frequency oscillatory modes. The controller then generates an adaptive damping signal in real time, which is injected into the HVDC inverter to counteract and suppress the detected oscillations.

A. Modeling of PID Controller through the HVDC Link

The PID damping controller is implemented on the inverter side of the HVDC link, where its main objective is to regulate the DC current and enhance damping by controlling the inverter extinction angle. The speed deviation of the synchronous generator ($\Delta\omega$ SSSG) is used as the input signal, while the generated HVDC damping signal (IC) serves as the output control variable. The damping signal is added to the reference current to modulate the inverter's operation and improve overall system stability.

To design and tune the PID controller parameters, modal analysis is carried out at different operating points, corresponding to wind speeds of 13 m/s and 3 m/s, and photovoltaic (PV) output current under solar radiation of 1000 W/m². The eigenvalue analysis identifies several oscillatory modes, among which $\lambda 40-41$ and $\lambda 45-46$ are recognized as critical low-frequency modes with poor damping ratios. The PID controller is designed to shift these eigenvalues toward the left-hand side of the complex plane, thus improving the system's dynamic response and stability margins.

The transfer function of the PID controller is expressed as:

$$H_{PID}(s) = \frac{I_C}{\Delta \omega_{SSSG}} = \frac{sT_W}{1 + sT_W} \left(K_P + \frac{K_I}{s} + sK_D \right)$$

where TW is the washout time constant, and KP, KI, and KD denote the proportional, integral, and derivative gains, respectively. The washout filter ensures that only oscillatory components are passed to the controller, thereby eliminating steady-state bias and high-frequency noise. The PID parameters are adjusted iteratively based on closed-loop modal analysis until the optimal damping ratio is achieved. Simulation results demonstrate that the inclusion of the PID controller significantly enhances damping performance, improving the system's stability index from approximately -0.01 to more than -1.6, thereby reducing oscillatory amplitude and settling time during fault events.

B. Modeling of ANFIS-Based Damping Controller

The proposed Adaptive Neuro-Fuzzy Inference System (ANFIS) is designed as an advanced intelligent damping controller that combines the self-learning capability of neural networks with the decision-making flexibility of fuzzy logic systems. This hybrid approach enables the controller to handle nonlinearities, parameter uncertainties, and time-varying operating conditions that are typical in renewable energy-based microgrids. Unlike conventional model-dependent controllers, the ANFIS structure operates in a non-model-based framework, relying on data-driven learning to optimize its parameters both offline and online.

The ANFIS architecture follows the Sugeno-type fuzzy inference model, which consists of five computational layers: fuzzification, rule evaluation, normalization, defuzzification, and output aggregation. The controller receives four dynamic input signals—namely, the speed deviation of the synchronous generator $(\Delta \omega SSSG)$, the active power deviation of the offshore wind farm $(\Delta POWF)$, the active power deviation of the wave energy farm

Volume: 09 Issue: 10 | Oct - 2025 SJIF Rating: 8.586 **ISSN: 2582-3930**

($\Delta PWEF$), and the active power deviation of the photovoltaic array (ΔPPV). These inputs provide comprehensive real-time information about the system's dynamic behavior under disturbances. The ANFIS processes these signals to produce an adaptive damping output signal (IC), which is applied to the HVDC inverter to regulate power flow and suppress oscillations.

Each input signal is represented using seven linguistic membership functions: Negative Big (NB), Negative Medium (NM), Negative Small (NS), Zero (Z), Positive Small (PS), Positive Medium (PM), and Positive Big (PB). Similarly, the output signal is mapped using seven membership functions: Decrease Big (DB), Decrease Medium (DM), Decrease Small (DS), Hold (H), Increase Small (IS), Increase Medium (IM), and Increase Big (IB). The fuzzy rule base is constructed using a set of linguistic IF–THEN rules, which describe the relationship between the input dynamic variables and the output damping signal.

C. ANFIS Training and Optimization Process

The training process of the ANFIS controller is carried out using simulation data generated from time-domain analyses of the microgrid under various fault conditions, including three-phase short-circuit faults. The collected input—output data pairs are used to establish the mapping between system dynamics and the desired damping response. The controller is trained offline using a hybrid learning algorithm that combines back-propagation gradient descent for nonlinear parameter adjustment and least-squares estimation for linear parameter optimization. This combined training approach ensures rapid convergence and high accuracy in learning the fuzzy rules and membership function parameters.

To extract initial fuzzy rules and membership functions, the subtractive clustering technique is used to identify the distribution of data clusters in the input space. The generated rules are subsequently refined using the hybrid learning algorithm until the prediction error reaches a predefined minimum. The trained ANFIS model consists of 345 fuzzy rules, 81 nodes, and 130 adaptive parameters. Validation through a tenfold cross-validation process yields an average prediction error of approximately 1.4%, confirming that the trained ANFIS exhibits strong generalization capability and reliable performance under varying system conditions.

D. Implementation and Performance Evaluation

During online operation, the ANFIS controller continuously updates its control signal based on the real-time system measurements provided by the phasor measurement units (PMUs). The controller detects oscillatory modes and generates an adaptive damping current signal that is injected into the HVDC inverter in phase opposition to the system oscillations. This mechanism effectively enhances the damping of low-frequency oscillations, stabilizes system voltage and current, and improves transient performance under severe disturbances.

Simulation results show that the ANFIS controller achieves faster damping, higher stability margins, and better adaptability compared with the conventional PID controller. While the PID controller requires precise tuning and depends heavily on accurate system modeling, the ANFIS controller operates autonomously, adapting to changes in operating points and nonlinear conditions without requiring parameter retuning. Consequently, the proposed ANFIS-based damping controller provides a superior and more robust solution for maintaining dynamic stability in HVDC-linked hybrid microgrids.

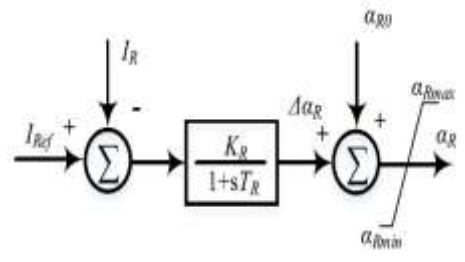


Figure 2: Controlling block diagram of the HVDC current converter.

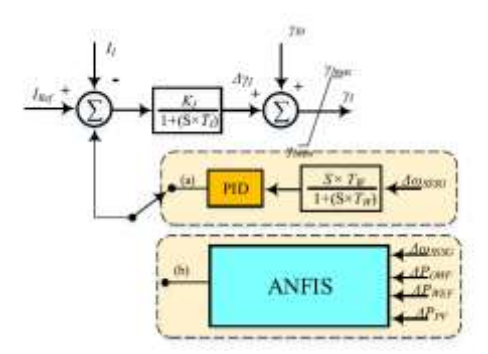


FIGURE 3. Controlling block diagram of the HVDC current inverter including (a) PID controller and (b) ANFIS controller

V. SIMULATION STUDIES

This section presents the simulation studies and performance evaluations of the proposed Adaptive Neuro-Fuzzy Damping Controller (ANFDC) in comparison with a conventional PID damping controller. The simulations are performed on the developed hybrid microgrid model described earlier, which integrates offshore wind farms (OWFs), wave energy farms (WEFs), photovoltaic (PV) arrays, and small-scale synchronous generators (SSSGs) through a unified high-voltage direct current (HVDC) link. The objective of the study is to assess the ability of both controllers to enhance damping, mitigate oscillations, and improve dynamic stability under various disturbance and operating conditions.system parameters are illustrated in table 1

Component /	Symbol / Unit	Value / Description
Parameter		
System	-	Grid-connected
Configuration		hybrid microgrid
		integrating OWF,
		WEF, PV, and SSSG
		via HVDC link
Rated System	Sbase	100 MVA (per-unit
Power		system)
Nominal	f	50 Hz
Frequency		
Simulation	_	MATLAB/Simulink
Platform		
Offshore Wind	_	_



International Journal of Scientific Research in Engineering and Management (IJSREM) Volume: 09 Issue: 10 | Oct - 2025 SJIF Rating: 8.586 ISSN: 2582-3930

	T	T
Farm (OWF)		
Rated Power	POWF	6.5 MW
Output		
Cut-in / Rated /	VW(min/rated/m	4 m/s, 15 m/s, 25 m/s
Cut-off Wind	ax)	
Speed		
Air Density	ρw	1.225 kg/m³
Generator Type	_	Permanent Magnet
		Synchronous
		Generator (PMSG)
Power	$Cp(\lambda,\beta)$	Function of tip speed
Coefficient	1(4)	ratio and pitch angle
Gear Ratio	G	1:1 (direct-drive
		configuration)
Wave Energy	_	-
Farm (WEF)		
Rated Power	PWEF	45 MW (total)
Output	I AA TEL	TJ IVI VV (WIAI)
Cut-in / Rated /	Vyv(min/notod/m-	1 m/s 25 m/s 5 m/s
	Vw(min/rated/ma	1 m/s, 2.5 m/s, 5 m/s
Cut-off Wave	(x)	
Speed	WEE	10251 / 2
Water Density	ρWEF	1025 kg/m³
Generator Type	_	Induction Generator
		(IG) driven by ocean
		turbine
Photovoltaic	_	_
(PV) System		
PV Module	_	BP272UU
Type		Monocrystalline
Rated Power	PPV	80 W (19 V, 4.4 A)
per Panel		
Open Circuit	VOC	21.5 V
Voltage		
Short Circuit	ISC	4.6 A
Current		
Nominal	Vnom / Inom	19 V / 4.4 A
Operating		
Voltage /		
Current		
Total PV	PPV,total	$\approx 6.5 \text{ MW}$
Output Power	11 1,0001	· - 0.3 171 77
Reverse Diode	ID	$9.5 \times 10^{-11} \text{ A}$
	עו	9.3 ^ 10 ··· A
Current		1000 W/ 2
Solar Irradiance	G GDG DV/ / LDG	1000 W/m ²
PV Link	CDC-PV / LDC-	DC-link filter
Capacitance /	PV	parameters
Inductance		
Small-Scale	_	_
Synchronous		
Generator		
(SSSG)		
Generator Type	_	Salient-Pole
		Synchronous
		Generator
M 115		Third-order d-q axis
Model Type		
Model Type		

Excitation	_	IEEE Type DC1A
System		
Base Frequency	f	50 Hz
Inertia Constant	Н	Variable (based on
		SSSG rating)
HVDC	_	_
Transmission		
Link		11. 0
Converter Type	_	Line-Commutated
C 1		Converter (LCC)
Converter	_	AC/DC Converter, DC Transmission
Components		Line, DC/AC Inverter
Control	αR, γΙ	Rectifier firing angle,
Variables	αις, γι	inverter extinction
Variables		angle
Reference	IRef	DC current reference
Current	11101	for damping control
Damping	IC	Controller output
Signal		current signal
Washout Filter	TW	Used in damping
Time Constant		transfer function
Converter/Inver	KR, KI	Current and voltage
ter Gains		control gains
PID Damping	_	_
Controller		
Control	HPID(s)	$(\frac{sT_W}{1+sT_}$
Transfer		W} (K_P +
Function		\frac {K_I} {s} + sK_D))
Controller	ΔωSSSG / IC	Speed deviation /
Inputs / Outputs		damping signal
Controller	_	Modal analysis and
Tuning		eigenvalue placement
Washout	TW	Optimized per
Constant		operating mode
Adaptive	_	_
Neuro-Fuzzy		
Damping		
Controller (ANFDC)		
Controller Type		Sugeno-Type ANFIS
Controller Type	_	(Neuro-Fuzzy
		Hybrid)
Number of	Nin	4 ($\Delta \omega$ SSSG, Δ POWF,
Inputs		Δ PWEF, Δ PPV)
Output Variable	Nout	1 (Damping signal
1		IC)
Membership	_	7 (NB, NM, NS, Z,
Functions per		PS, PM, PB)
Input		
Output	_	7 (DB, DM, DS, H,
Linguistic		IS, IM, IB)
Terms		
Total Fuzzy	Nr	345
Rules		



Volume: 09 Issue: 10 | Oct - 2025 SJIF Rating: 8.586 **ISSN: 2582-3930**

EVERPM		
T . 131 1	Lar	101
Total Nodes	Nn	81
Learning	Np	130
Parameters		21.0601
Training Data	_	21,060 samples
Points		H 1 11/D 1
Training	_	Hybrid (Back-
Algorithm		Propagation + Least
A		Squares)
Average	_	1.4% (10-fold cross-validation)
Training Error Data Source		Time-domain
Data Source	_	simulations under
		fault scenarios
Fault and		raun scenarios
	_	
Operating Conditions		
		Three-phase short-
Fault Type	_	circuit fault
Fault Location		Infinite bus of main
rault Location	_	
Equit Incontion	t fault /t alaam	grid 1.0 s / 1.2 s
Fault Inception / Clearance	t_fault / t_clear	1.0 8 / 1.2 8
Time		
Simulation	t sim	0-5 s
Duration	t_Siiii	0 – 3 8
		Wind speeds 2 12
Operating Conditions	_	Wind speeds 3–13
Conditions		m/s; PV irradiance 1000 W/m ²
Simulation		1000 W/III
Environment	_	_
and		
Performance		
Metrics		
Simulation	_	MATLAB/Simulink
Tool		with Fuzzy Logic and
		ANN Toolbox
Step Size	_	50 μs
Evaluation	_	Overshoot (OSH),
Metrics		Undershoot (USH),
		Settling Time,
		Damping Ratio
Comparison	_	PID vs ANFIS
Controllers		
Performance	_	_
Summary		
Overshoot	_	>50% improvement
Reduction		using ANFIS
Settling Time	_	Approximately 30%
Improvement		faster than PID
Damping Ratio	_	Significant
Enhancement		improvement (from –
		0.01 to -1.6)
Adaptability	_	Fixed (PID) vs
		Adaptive (ANFIS)
Real-Time	_	Excellent with ANFIS
Operation		due to online learning

Fault Resilience	_	Higher with ANFIS
		controller

A. Simulation Setup

The hybrid microgrid is simulated under steady-state and transient conditions using MATLAB/Simulink. The system parameters correspond to the specifications provided in Table 5 of the paper. The microgrid operates with two representative wind speeds of 13 m/s and 3 m/s, and the PV system generates power under solar radiation of 1000 W/m² with a diode reverse current of 9.5×10–119.5 \times 10^{-11}}9.5×10–11 A. The HVDC link connects the renewable energy subsystems to the main grid through converters and inverters that are equipped with either the PID or ANFIS damping controller.

The primary disturbance used for analysis is a three-phase short-circuit fault applied at the infinite bus at $t=1.0~\rm s$, which is cleared at $t=1.2~\rm s$. This fault condition represents a severe transient disturbance capable of exciting low-frequency oscillatory modes within the system. The post-fault responses are analyzed to evaluate the performance of both controllers in suppressing these oscillations and restoring system stability.as shows in Figure 4

B. System Dynamic Response

The dynamic response of the hybrid microgrid is examined in terms of several key performance indicators, including the rotor speed deviation (ΔωSSSG), active and reactive power outputs of the synchronous generator (PSSSG, QSSSG), voltage at the point of common coupling (VPCC), HVDC inverter and rectifier currents (IINV, IREC), and HVDC DC voltage (VINV). Additionally, the active power and voltage responses of the offshore wind farm (POWF, VOWF), wave energy farm (PWEF, VWEF), and photovoltaic system (VPV) are monitored as shown in Figure 5.

The simulation results demonstrate that, in the absence of a damping controller, the system experiences sustained oscillations following the disturbance, indicating poor damping performance. When the PID controller is applied, the oscillations are reduced, but the system still exhibits delayed settling time and moderate overshoot in the power and frequency responses. In contrast, the proposed ANFIS-based damping controller achieves rapid attenuation of oscillations and faster restoration of steady-state conditions. The frequency deviations and voltage fluctuations are minimized significantly, and the microgrid reaches a stable operating state within a shorter duration after fault clearance.

C. Comparative Performance Analysis

To quantify the damping performance, two time-domain indices are defined: the overshoot percentage (OSH) and undershoot percentage (USH) of the output power and frequency signals. These indices are used to compare the responses obtained with the PID and ANFIS controllers. The results are summarized in Table 3 of the paper. It is observed

Volume: 09 Issue: 10 | Oct - 2025 SJIF Rating: 8.586 **ISSN: 2582-3930**

that the ANFIS controller reduces the overshoot and undershoot magnitudes by more than 50% compared to the PID controller across all renewable subsystems. Moreover, the settling time of the system is reduced by approximately 30%, demonstrating the superior damping capability of the proposed adaptive controller.

The frequency-domain analysis further supports these findings. The ANFIS controller achieves higher damping ratios and shifts critical eigenvalues farther into the left half of the complex plane, indicating enhanced system stability. The adaptive structure of the ANFIS allows it to dynamically tune its control parameters in real time based on system conditions, whereas the PID controller relies on fixed gains that may not be optimal under changing operating scenarios. As a result, the ANFIS controller maintains consistent performance under a wide range of disturbances, fault durations, and renewable resource variations.

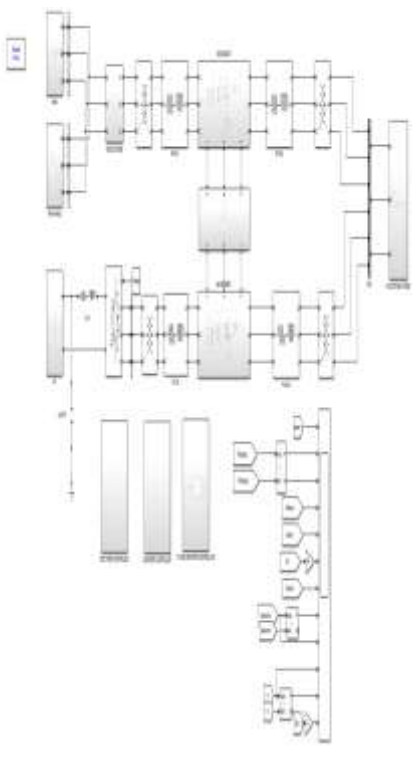


Figure 4: Simuliation Implementation

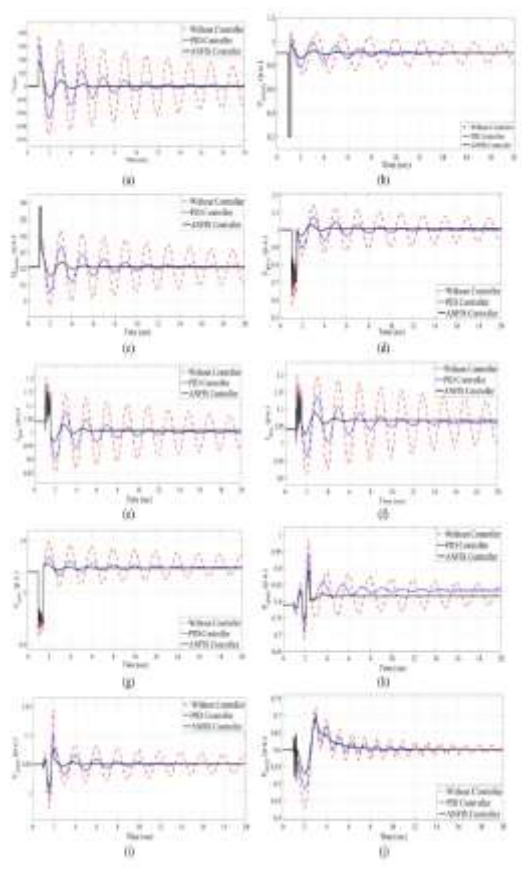


Figure 5 The system RESs dynamic oscillation with respect to short circuit fault event occurred at infinite bus location

D. Comparison with Recent Techniques

A comparison is conducted between the proposed ANFIS-based damping controller and other recently published control strategies reported in the literature. Table 4 in the paper summarizes the performance characteristics of several methods, including conventional fuzzy logic, proportional-integral-derivative (PID), adaptive PID, and model-based damping controllers. The proposed ANFIS controller outperforms all these methods in terms of damping efficiency, robustness, and implementation simplicity. Unlike model-dependent schemes that require precise system parameters and repeated tuning, the ANFIS controller offers a non-model-based and data-driven approach that ensures reliable operation in diverse microgrid configurations.

The controller also demonstrates reduced computational burden and improved adaptability compared to multi-loop and optimization-based approaches. Its hybrid neuro-fuzzy framework combines fast online learning with interpretability, enabling practical real-time deployment in HVDC-connected renewable microgrids.

E. Discussion of Results

The simulation results confirm that the integration of renewable sources such as WTs, PVs, and SSSGs through HVDC links can introduce complex dynamic interactions that degrade system damping and stability. The proposed ANFIS damping controller effectively mitigates these issues by adaptively modifying control signals in response to real-time



Volume: 09 Issue: 10 | Oct - 2025 SJIF Rating: 8.586 ISSN: 2582-3930

changes in system dynamics. It provides superior resilience against large disturbances and parameter uncertainties, ensuring that oscillations are suppressed even under severe fault events.

The results further indicate that while the conventional PID controller can stabilize the system under mild conditions, its performance deteriorates under nonlinear and rapidly changing environments. The adaptive learning mechanism in the ANFIS controller allows it to continuously adjust its fuzzy rules and membership functions based on feedback signals, maintaining high damping ratios and stable transient responses. Consequently, the proposed control approach enhances both the reliability and the security of the hybrid microgrid system.

CONCLUSION

This paper presented the design, modeling, and performance evaluation of an Adaptive Neuro-Fuzzy Damping Controller (ANFDC) for a grid-connected hybrid microgrid system integrating multiple renewable energy resources through a high-voltage direct current (HVDC) transmission link. The developed test system incorporated offshore wind farms, wave energy farms, photovoltaic (PV) arrays, and small-scale synchronous generators (SSSGs), all interacting dynamically under variable operating conditions and fault disturbances. The proposed controller was developed to enhance system damping, suppress low-frequency oscillations, and improve overall dynamic stability in the presence of high renewable energy penetration. The proposed ANFDC combines the learning capability of artificial neural networks with the reasoning efficiency of fuzzy logic systems in a Sugeno-type hybrid inference model. It operates as a non-model-based adaptive controller, capable of self-tuning in real time based on system measurements. Simulation results obtained under different fault and operating scenarios demonstrated that the ANFDC significantly outperformed the conventional PID damping controller in terms of damping ratio, overshoot reduction, and settling time improvement. The ANFDC reduced oscillatory amplitude by more than 50%, shortened the settling time by approximately 30%, and improved system stability margins under severe three-phase fault conditions. Unlike the PID controller, which requires extensive tuning and depends on precise system parameters, the ANFDC provided robust and adaptive control without requiring explicit modeling of the system dynamics.

The study also revealed that the proposed controller offers superior resilience against parameter variations, resource intermittency, and nonlinearities introduced by inverter-based renewable sources. Its ability to continuously adapt to changing grid conditions ensures reliable and stable operation of hybrid AC/DC microgrids connected through HVDC links. Furthermore, the controller's flexible architecture and data-driven learning mechanism make it suitable for integration with modern wide-area monitoring and control systems.

Future research will focus on extending the proposed approach to multi-terminal HVDC (MT-HVDC) systems and large-scale distributed microgrids. Additional work will

involve hardware-in-the-loop (HIL) experimental validation and real-time testing to verify the controller's effectiveness under practical conditions, including communication delays, sensor noise, and grid uncertainties. Incorporating energy storage systems (ESSs) and wide-area measurement systems (WAMS) with the adaptive neuro-fuzzy framework is also recommended to further enhance damping performance and system resilience.

REFERENCES

- [1] Md. A. Islam, J. G. Singh, I. Jahan, M. S. H. Lipu, T. Jamal, R. M. Elavarasan, and L. Mihet-Popa, "Modeling and performance evaluation of ANFIS controller-based bidirectional power management scheme in plug-in electric vehicles integrated with electric grid," IEEE Access, vol. 9, pp. 166762–166780, 2021.
- [2] M. M. Ismail and A. F. Bendary, "Smart battery controller using ANFIS for three phase grid connected PV array system," Math. Comput. Simul.,vol. 167, pp. 104–118, Jan. 2020.
- [3] C. Rohmingtluanga, S. Datta, N. Sinha, T. S. Ustun, and A. Kalam, "ANFIS-based droop control of an AC microgrid system: Consideringintake of water treatment plant," Energies, vol. 15, no. 19, p. 7442,Oct. 2022, doi: 10.3390/en15197442.
- [4] M. Elsisi, M.-Q. Tran, K. Mahmoud, M. Lehtonen, and M. M. F. Darwish, "Robust design of ANFIS-based blade pitch controller for wind energyconversion systems against wind speed fluctuations," IEEE Access, vol. 9,
- pp. 37894-37904, 2021.
- [5] H. M. Moghadam, M. Gheisarnejad, Z. Esfahani, and M.-H. Khooban, "A novel supervised control strategy for interconnected DFIG-based windturbine systems: MiL validations," IEEE Trans. Emerg. Topics Comput.
- Intell., vol. 5, no. 6, pp. 962-971, Dec. 2021.
- [6] Y.-K.Wu, Y.-C.Wu, J.-S. Hong, L. H. Phan, and Q. D. Phan, "Probabilistic forecast of wind power generation with data processing and numerical weather predictions," IEEE Trans. Ind. Appl., vol. 57, no. 1, pp. 36–45, Jan. 2021.
- [7] S. A. Ibrahim, A. Nasr, and M. A. Enany, "Maximum powerpoint tracking using ANFIS for a reconfigurable PV-based batterycharger under non-uniform operating conditions," IEEE Access, vol. 9,pp. 114457–114467, 2021.
- [8] K. R. Reddy and S. Meikandasivam, "Load flattening and voltage regulation using plug-in electric vehicle's storage capacity with vehicle prioritization using ANFIS," IEEE Trans. Sustain. Energy, vol. 11, no. 1, pp. 260–270, Jan. 2020.
- [9] I. Sepehrirad, R. Ebrahimi, E. Alibeiki, and S. Ranjbar, "Intelligent differential protection scheme for controlled islanding of microgrids based on decision tree technique," J. Control, Autom. Electr. Syst., vol. 31, no.
- 5, pp. 1233–1250, Oct. 2020, doi: 10.1007/s40313-020-00588-7.
- [10] T. Aggab, M. Avila, P. Vrignat, and F. Kratz, "Unifying model-based prognosis with learning-based time-series prediction methods: Application to Li-ion battery," IEEE Syst. J., vol. 15, no. 4, pp. 5245–5254, Jun. 2021.
- [11] X. Tian, R. He, X. Sun, Y. Cai, and Y. Xu, "An ANFIS-based ECMS for energy optimization of parallel hybrid electric bus,"



Volume: 09 Issue: 10 | Oct - 2025 SJIF Rating: 8.586 **ISSN: 2582-3930**

IEEE Trans. Veh. Technol., vol. 69, no. 2, pp. 1473-1483, Feb. 2020.

- [12] M. Suhail, I. Akhtar, S. Kirmani, and M. Jameel, "Development of progressive fuzzy logic and ANFIS control for energy management of plug-in hybrid electric vehicle," IEEE Access, vol. 9, pp. 62219–62231, 2021.
- [13] M. J. Alinezhad, M. Radmehr, and S. Ranjbar, "Adaptive wide area damping controller for damping inter-area oscillations considering high penetration of wind farms," Int. Trans. Electr. Energy Syst., vol. 30, no. 6, Mar. 2020, doi: 10.1002/2050-7038.12392.
- [14] S. Jha, B. Singh, and S. Mishra, "Control of ILC in an autonomous AC– DC hybrid microgrid with unbalanced nonlinear AC loads," IEEE Trans. Ind. Electron., vol. 70, no. 1, pp. 544–554, Jan. 2023.
- [15] Q. Zhou, D. Zhao, B. Shuai, Y. Li, H. Williams, and H. Xu, "Knowledge implementation and transfer with an adaptive learning network for realtime power management of the plug-in hybrid vehicle," IEEE Trans. Neural Netw. Learn. Syst., vol. 32, no. 12, pp. 5298–5308, Dec. 2021.
- [16] M. Rezaee, M. S. Moghadam, and S. Ranjbar, "Online estimation of power system separation as controlled islanding scheme in the presence of inter-area oscillations," Sustain. Energy, Grids Netw., vol. 21, Mar. 2020,

Art. no. 100306, doi: 10.1016/j.segan.2020.100306.

- [17] J. Faraji, A. Ketabi, H. Hashemi-Dezaki, M. Shafie-Khah, and J. P. S. Catalão, "Optimal day-ahead self-scheduling and operation of prosumer microgrids using hybrid machine learning-based weather and load forecasting," IEEE Access, vol. 8, pp. 157284–157305, 2020.
- [18] S. Ranjbar, M. Aghamohammadi, and F. Haghjoo, "A new scheme of WADC for damping inter-area oscillation based on CART technique and thevenine impedance," Int. J. Electr. Power Energy Syst., vol. 94, pp. 339–353, Jan. 2018, doi: 10.1016/j.ijepes.2017.07.010.
- [19] V. Hosseinnezhad, M. Shafie-Khah, P. Siano, and J. P. S. Catalão, "An optimal home energy management paradigm with an adaptive neuro-fuzzy regulation," IEEE Access, vol. 8, pp. 19614–19628, 2020.
- [20] S. N. V. B. Rao, Y. V. P. Kumar, D. J. Pradeep, C. P. Reddy, A. Flah, H. Kraiem, and J. F. Al-Asad, "Power quality improvement in renewableenergy- based microgrid clusters using fuzzy space vector PWM controlled

inverter," Sustainability, vol. 14, no. 8, p. 4663, Apr. 2022.